Semicond. Sci. Technol. **27** (2012) 085015 (5pp) doi:10.1088/0268-1242/27/8/085015

Electrical properties of quasi-vertical Schottky diodes

W Witte[1], D Fahle[1], H Koch[1], M Heuken[1,2], H Kalisch[1] and A Vescan[1]

[1] GaN Device Technology, RWTH Aachen University, 52074 Aachen, Germany
[2] AIXTRON SE, 52134 Herzogenrath, Germany

E-mail: witte@gan.rwth-aachen.de

Received 22 March 2012, in final form 12 June 2012
Published 11 July 2012
Online at stacks.iop.org/SST/27/085015

Abstract
In this paper, we report on quasi-vertical Schottky diodes on GaN on sapphire focusing on the influence of Ni/Au Schottky contact annealing and the doping concentration of the n-GaN onto their electrical properties. Schottky contact annealing is shown to improve the metal–semiconductor interface, as reflected in reduced ideality factor and increased barrier height. Additionally, a decrease of leakage currents and a drastic improvement of the breakdown field are achieved. The annealing temperature is shown to have an optimum value around 400 °C beyond which the device degrades. Further reduction of reverse leakage currents and an increase in breakdown voltage are achieved by decreasing the doping concentration in the n-GaN epitaxial layer. So far, a doping concentration of 2×10^{16} cm^{-3} showed the best results in terms of series resistance and breakdown behavior with $R_{on} = 1$ mΩ cm^2 and $V_{Br} = 230$ V.

(Some figures may appear in colour only in the online journal)

1. Introduction

Wide bandgap semiconductors such as gallium nitride (GaN) have recently become an active field of research because of their suitability for high-power, high-voltage and high-temperature applications [1]. Since the estimated critical electrical field for GaN is 3 MV cm^{-1} and therefore ten times higher than that of silicon, this material system may substitute silicon in several application areas [2].

Therefore, vertical Schottky diodes of GaN are of great interest. They can handle high voltages [3] because of their unipolar nature, they show a fast reverse recovery and switching speed [4]. Also, packaging and thermal management become easier in a vertical configuration.

To realize Schottky diodes which can fully exploit the potential advantages of the nitride material system, it is necessary to have a fundamental understanding of the mechanisms which dominate the electronic properties of the device. Several investigations of Ni Schottky diodes on n-GaN have been performed, studying the behavior of barrier height, ideality factor and leakage currents [5–10].

In this paper, we not only study the forward characteristics of quasi-vertical Schottky diodes, but also turn our attention to the reverse characteristics, in particular, to the breakdown behavior. Therefore, we investigate the dependence of the reverse blocking characteristics on contact annealing and vertical layer design. Here, we focused on the impact of the doping concentration on the diode characteristics.

As the standard substrate sapphire is insulating, vertical Schottky diodes require a GaN substrate or backside processing such as substrate removal or via technology [11]. Both options are to date still prohibitively expensive. In order to be able to investigate the basic properties of a vertical design, we fabricated quasi-vertical devices, with the backside contact provided by a highly doped buffer layer.

2. Experimental details

As mentioned before, two series of experiments were performed. In series A, the annealing temperature of the Schottky contact on n$^-$-GaN was optimized. To investigate the influence of the epitaxial layer on the diode characteristics, in series B, diodes with different doping concentrations of the n$^-$-GaN region were fabricated.

For both series, the GaN layers were grown on c-plane sapphire by metal organic vapor phase epitaxy, using TMGa,

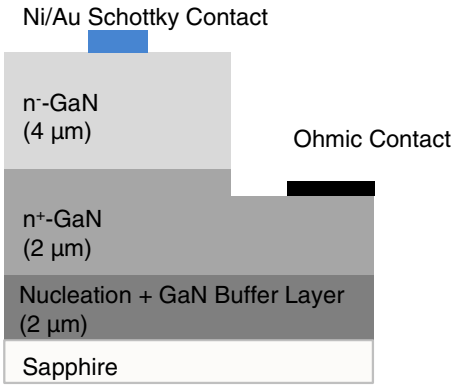

Figure 1. Schematic cross-sectional view of a vertical Schottky diode.

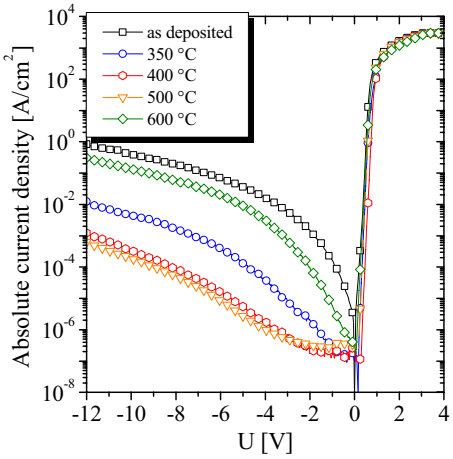

Figure 2. *I–V* characteristics of vertical Schottky diodes for different annealing temperatures.

NH_3 and SiH_4 as precursors. The growth was started with a 2 μm nominally undoped GaN buffer layer and continued with a 2 μm n^+-GaN layer (doping level: 1×10^{18} cm^{-3}) for the backside contact.

For series A, this was followed by 4 μm n^--GaN with a doping concentration of 1.2×10^{17} cm^{-3}. For series B, various doping levels of the n^--GaN, ranging from unintentionally doped (UID) to 2.2×10^{16} cm^{-3} and 6×10^{16} to 1.2×10^{17} cm^{-3}, were fabricated by varying the SiH_4 flow.

The dislocation density of the epilayer was estimated from the FWHM of the (0 0 0 2) and (10–12) XRD reflex to approx. 1×10^9 cm^{-2}. This value was independent of doping concentration.

Mesa structures were formed by $BCl_3/Cl_2/N_2$ inductively coupled plasma reactive ion etching (300 W source power, 200 W RF power) using Ni as hard-mask material. An etch depth of slightly more than 4 μm was targeted in order to expose the n^+-buffer.

Before metal deposition, the samples were dipped 1 min in HCl:H_2O (1:1) etchant and rinsed with deionized water afterwards. Ti/Al/Ni/Au (15 nm/100 nm/40 nm/50 nm) ohmic contacts were deposited on the etched surface via electron beam evaporation and subsequently annealed at 650 °C under N_2 ambient. Finally, Ni/Au (50 nm/200 nm) Schottky contacts were deposited on top of the mesas (figure 1).

The fabricated diodes, with a diameter of 33 μm, of both series were characterized by *I–V* and *C–V* measurements to analyze ideality factor, barrier height and reverse blocking properties. Also, breakdown characteristics were investigated.

For series A, the samples were analyzed as deposited and also after annealing performed under N_2 ambient for 10 min at 350 °C, 400 °C, 500 °C and 600 °C, respectively. Samples of series B were annealed at 400 °C and characterized thereafter.

3. Results and discussion

3.1. Series A: Schottky contact annealing

First, the ohmic contacts of the fabricated devices were characterized by circular TLM [12]. Ohmic properties were confirmed and the specific contact resistivity was extracted as 4.7×10^{-6} Ω cm^2.

The *I–V* characteristics of the quasi-vertical Schottky diodes for different annealing temperatures are shown in figure 2.

As-deposited Schottky contacts on n-GaN show relatively high reverse leakage currents, up to 1 A cm^{-2} at a bias of −12 V, as was also reported by [6]. Annealing of the contacts from 350 °C up to 500 °C continuously reduces the reverse diode current by up to three orders of magnitude. For higher temperatures, we observe a degradation of the reverse blocking properties which is also accompanied by a roughening of the Schottky contact metallization and the formation of hillock-like structures. This could be related to the formation of Ni–Ga compounds, as previously reported by Montayed *et al* for annealing above 600 °C [5].

A more detailed analysis of the forward characteristics allows us to extract the ideality factor and barrier height according to the simple thermionic emission theory:

$$I = AA^*T^2 e^{-\frac{\Phi_B}{kT}} \left(e^{-\frac{eV}{nkT}} - 1\right) \quad (1)$$

in which A is the diode area, $A^* = 26.4$ A cm^{-2} K^2 is the Richardson constant [13], T the temperature, Φ_B the barrier height, V the applied voltage, k is Boltzmann's constant and n is the ideality factor.

The results are summarized in figure 3, in which we show the average values extracted from several measurements across the sample. It is found that the ideality factor n systematically decreases for annealing temperatures up to 500 °C, from $n = 1.15$ to $n = 1.07$. Also, we observe an increase of the extracted Schottky barrier height and a reduction of reverse leakage currents. These trends indicate that the quality of the metal–semiconductor interface is improving and thermionic emission over a more homogeneous Schottky barrier is becoming dominant [14]. Note that an inhomogeneous Schottky barrier height distribution, e.g. due to interfacial oxide or interface states, at the metal–semiconductor interface may become apparent in a higher ideality factor [14].

The barrier height however decreases already at an annealing temperature of 500 °C, which may be due to the first interfacial reactions. This becomes also visible in the morphology as mentioned above. The values of the ideality

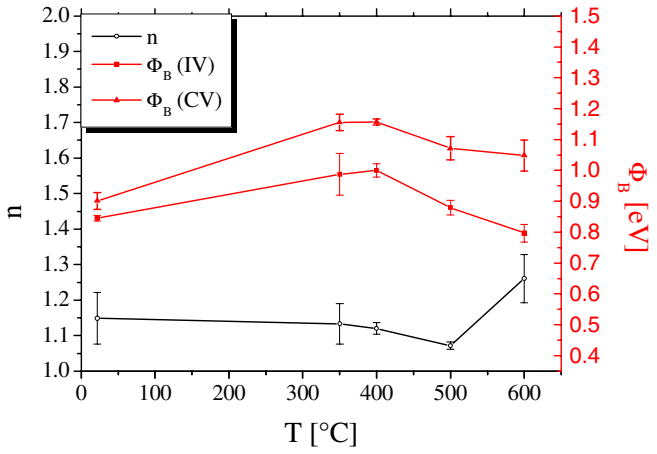

Figure 3. Dependence of the ideality factor n and the barrier height Φ_B on the annealing temperature.

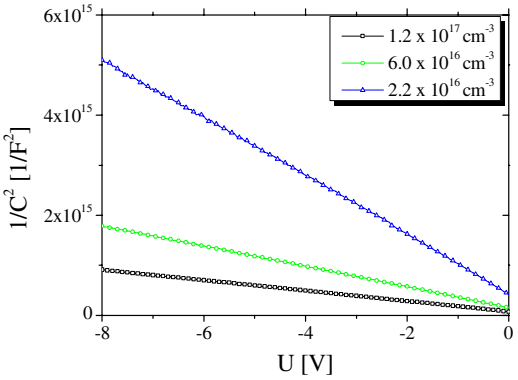

Figure 4. The linearity of the $1/C^2$ plot confirms that the doped samples have a homogeneous doping profile.

factor and the barrier height degrade further as the annealing temperature reaches 600 °C.

The barrier height was also determined from *C–V* measurements performed at 1 MHz. As the doping density is reasonably constant near the surface, we can extract the built-in voltage V_{bi} from a $1/C^2$ versus V plot.

The barrier height was then determined according to

$$\phi_B = -V_{\mathrm{bi}} + V_0 + \frac{kT}{q}, \tag{2}$$

with

$$V_0 = \frac{kT}{q} \ln\left(\frac{N_c}{N_D}\right) \tag{3}$$

and $N_c = 2.38 \times 10^{18}$ cm^{-2} [15] as the effective density of states in the conduction band and the doping density N_D extracted from the slope of the $1/C^2$ plot.

The *C–V* barrier heights are systematically about 0.2 eV higher than those from the *I–V* characteristics (figure 3). The overall trend as a function of annealing temperature is the same as for the *I–V* measurements. The higher values for the *C–V* results can be easily explained by the fact that the *C–V* measurements are less sensitive to the contribution of low barrier-height regions, whereas forward current measurements naturally include the leakage contribution of these regions affecting the extracted barrier height more severely.

The reverse blocking characteristics for different annealing temperatures were also investigated. The voltage at which the destructive breakdown occurs is defined as the breakdown voltage. For the non-annealed sample, the breakdown voltage is $V_{\mathrm{Br}} = 25$ V, with an average doping concentration of 1.2×10^{17} cm^{-3}, calculated from the *C–V* measurements. With

$$E_C = \frac{2(V_{\mathrm{bi}} - V_{\mathrm{Br}} - kT/q)}{w}, \tag{4}$$

the critical electric field is determined, with w as space charge region width, to ∼1 MV cm^{-1}. After annealing the sample up to 400 °C, the breakdown voltage increases to 55 V and the critical electric field to 1.5 MV cm^{-1}. Since annealing should not affect the GaN bulk properties, the latter is an indication that the breakdown is dominated at least partially by the inhomogeneous contact regions with lower barrier height. This effect appears to be reduced with annealing. On the other hand, the breakdown field is still significantly lower than the theoretical value of 3 MV cm^{-1}. Here, the dislocation density and damage introduced by mesa etching at the contact periphery may lead to a premature breakdown. Edge terminations as shown in [16] may suppress surface leakage contributions and the maximum field at contact edges.

3.2. Series B: variation of doping concentration

Prior to the characterization of the samples from series B, Schottky contact annealing was performed based on the results of the previous section. The annealing temperature was chosen as 400 °C. From *C–V* measurements performed at 1 MHz, the doping concentrations were determined to be 1.2×10^{17}, 6.0×10^{16} and 2.2×10^{16} cm^{-3}, respectively. The $1/C^2$ plot (figure 4) shows that all doped samples have reasonably constant doping levels throughout the profiled depth.

The carrier concentration of the UID sample was too low to be determined. The measured capacitance was constant throughout the voltage bias range from −8 V to +2 V. We assume therefore that the layer is completely depleted or even compensated. The total thickness was extracted from the capacitance of about 3.9 μm, which corresponds perfectly to the nominal n$^-$-GaN thickness.

The impact of the doping concentration can impressively be seen in the *I–V* behavior, especially for the reduction of the reverse leakage currents (figure 5). Also, the performance of the diode in the forward direction changes with doping.

By applying (1), we can extract the ideality factor and the barrier height (figure 6). The intentionally doped samples show the expected diode characteristics. The sample with the lowest doping concentration yields an ideality factor as low as 1.01. With higher doping concentration, n increases and at the same time Φ_B decreases.

Higher doping normally leads to larger contributions of tunneling currents and also image force barrier lowering due to the shift of the Fermi level.

Since the trend of decreasing barrier height is also exactly reproduced for the values extracted from *C–V* measurements,

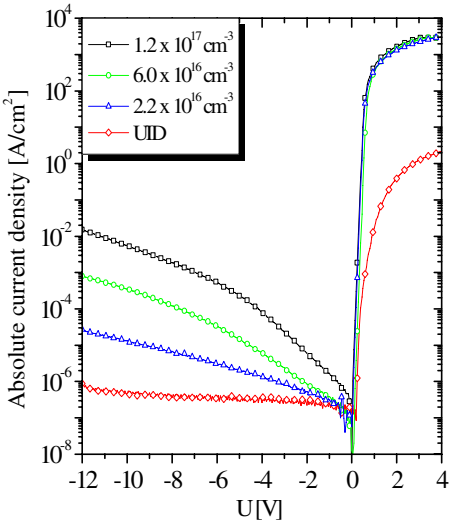

Figure 5. *I–V* characteristics of vertical Schottky diodes for different n^- doping concentrations.

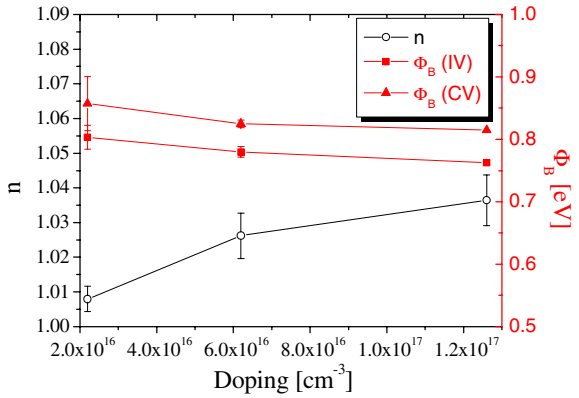

Figure 6. Barrier height, calculated from *I–V* and *C–V* measurements, and ideality factor with doping concentration.

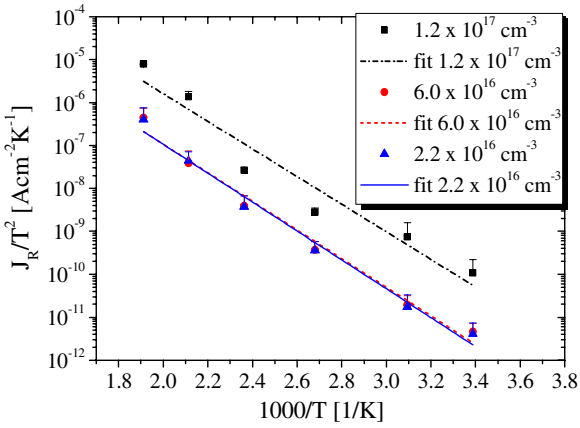

Figure 7. Arrhenius plot of the vertical leakage currents J_R/T^2 shows a linear correlation.

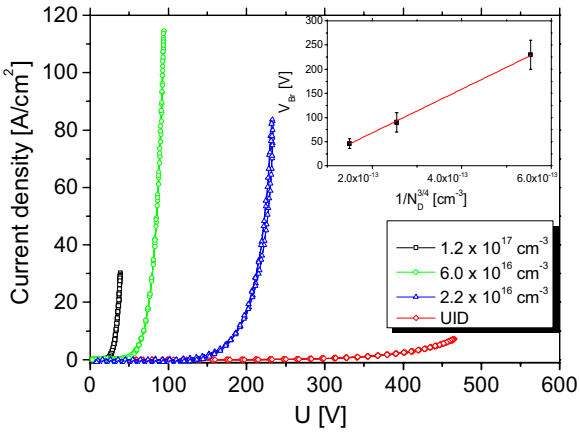

Figure 8. Reverse characteristics of vertical Schottky diodes with respect to the doping concentration in the n^--GaN region. Inset: $1/N_D^{3/4}$ behavior of the breakdown voltage.

which should not be affected by these effects, the same root cause is assumed to be responsible for the variation in barrier height and ideality factor. Defects or strain due to the silicon doping may affect the diode characteristics. Additional analysis, including variation of layer thicknesses, for example, could shed some light on this.

By studying the temperature dependence of the reverse leakage currents, we can gain more information about the barrier height dominating current transport in this bias regime. The reverse leakage currents J_R were measured in a temperature range from room temperature to 250 °C. Plotting J_R/T^2 at -2 V over $1/T$ shows linear behavior (figure 7) in a semi-log plot.

Using the relationship introduced in [10]

$$J_R = A * T^2 \left(e^{-\frac{q}{kT}\Phi_B}\right)\left(e^{\frac{q}{kT}\Delta\Phi_B}\right)\left(e^{c_T E_M^2}\right), \qquad (5)$$

with $\Delta\Phi_B$ as the reduction of the Schottky barrier due to image force barrier lowering, c_T as tunneling coefficient and E_M as the maximum electric field applied at the metal semiconductor interface, we can calculate the effective barrier height. With increasing doping concentration, the slope increases as well, this means according to (5) that the effective barrier height is reduced due to image force barrier lowering. Barrier heights of about 0.28 eV, similar to the values extracted by Ozbek *et al* [10], were calculated. This low value confirms the assumption of inhomogeneity of the Schottky barrier.

No reasonable value for barrier height or ideality factor can be extracted for the UID sample. Since the capacitance measurement implies a fully depleted n-layer, we could assume the conduction mechanism to be partially space-charge limited. A much more precise analysis is required though.

To minimize losses during device operation in the forward direction, low series resistances are required. For our doped Schottky diodes, we obtained values in the 0.8–1.0 mΩ cm^2 range for diodes with 33 μm diameter. As expected, the series resistance increases with lower doping concentration. For the UID sample, the extracted series resistance was found to be about 1 Ω cm^2.

The breakdown characteristics were also investigated in dependence of the doping concentration (figure 8).

A systematic increase of breakdown voltage with lower doping concentration is observed. The behavior follows quite

Table 1. Measured breakdown voltages and their corresponding calculated breakdown fields.

N_D (cm^{-3})	V_{Br} (V)	E_C (MV cm^{-1})
1.2×10^{17}	50	1.43
6.0×10^{16}	110	1.52
2.2×10^{16}	230	1.33
UID	460	2.35 (1.17)

well the dependence

$$V_{Br} \sim \frac{1}{N_D^{3/4}}, \tag{6}$$

predicted by Trivedi *et al* [17] (see inset in figure 8).

From the breakdown voltage V_{Br}, the critical electric field can be calculated with (4). Breakdown voltages and resulting critical fields, assuming constant doping concentration of the n$^-$-GaN region for simplicity, are listed in table 1.

The extracted data for the breakdown field show no significant variation with doping density. This effect is somewhat surprising, as it does not correlate with *I–V* characteristics data or barrier heights. The UID sample yields a breakdown field of 2.35 MV cm^{-1} if we apply also (4) and use the thickness $w = 3.9$ μm as determined from capacitance measurements before. However, this value is almost twice as high as for the other samples and should be treated with care. On the other hand, if we assume that the UID sample is fully compensated and the voltage drops linearly across the whole n$^-$-GaN thickness, the breakdown field is only 1.17 MV cm^{-1} and quite similar to those of the other diodes.

Intentional and controlled low-level doping experiments should reveal interesting aspects of the conduction mechanism in GaN Schottky diodes and help explain this behavior.

4. Conclusion

In order to obtain a fundamental understanding of the electrical behavior of vertical Schottky diodes, we investigated the influence of Schottky contact annealing and the doping concentration of the n$^-$-GaN layer.

We found that Schottky contact annealing at 400 °C for 10 min shows a pronounced reduction in leakage currents of three orders of magnitude and as well leads to an enhancement of the critical electric field from 0.99 to 1.5 MV cm^{-2}. This is linked to the improvement in metal–semiconductor interface quality.

Reducing the doping concentration of the n$^-$-GaN region to 2.2×10^{16} cm^{-3} shows further improvement in terms of reverse leakage currents and breakdown voltage. At this low doping concentration, diodes had series resistances of only 1 mΩ cm^2 and reasonable breakdown voltages of 230 V. Nevertheless, the critical electrical field does not increase with lower doping. This is probably caused by defects generated in the nucleation or n$^+$-layer, which penetrate throughout the layer.

Acknowledgment

The authors acknowledge financial support by BMBF (13N10913).

References

[1] Chow T P and Tyagi R 1994 Wide bandgap compound semiconductors for superior high-voltage unipolar power devices *IEEE Trans. Electron Devices* **41** 1481–3
[2] Bandic Z Z, Bridger P M, Piquette E C, McGill T C, Vaudo R P, Phanse V M and Redwing J M 1999 High voltage (450 V) GaN Schottky rectifiers *Appl. Phys. Lett.* **74** 1266–8
[3] Wang Y *et al* 2011 Ultra-low leakage and high breakdown Schottky diodes fabricated on free-standing GaN substrate *Semicond. Sci. Technol.* **26** 022002
[4] Zhou Y, Li M, Wang D, Ahyi C, Tin C-C, Williams J, Park M, Williams N M and Hanser A 2006 Electrical characteristics of bulk GaN-based Schottky rectifiers with ultrafast reverse recovery *Appl. Phys. Lett.* **88** 113509
[5] Motayed A, Davydov A V, Bendersky L A, Wood M C, Derenge M A, Wang D F, Jones K A and Mohammad S N 2002 High-transparency Ni/Au bilayer contacts to n-type GaN *J. Appl. Phys.* **92** 5218–27
[6] Miura N, Nanjo T, Suita M, Oishi T, Abe Y, Ozeki T, Ishikawa H, Egawa T and Jimbo T 2004 Thermal annealing effects on Ni/Au based Schottky contacts on n-GaN and AlGaN/GaN with insertion of high work function metal *Solid State Electron.* **48** 689–95
[7] Yildirim N, Ejderha K and Turut A 2010 On temperature-dependent experimental *I–V* and *C–V* data of Ni/n-GaN Schottky contacts *J. Appl. Phys.* **108** 114506
[8] Guo J D, Pan F M, Feng M S, Guo R J, Chou P F and Chang C Y 1996 Schottky contact and the thermal stability of Ni on n-type GaN *J. Appl. Phys.* **80** 1623–7
[9] Zhang B J, Egawa T, Zhao G Y, Ishikawa H, Umeno M and Jimbo T 2001 Schottky diodes of Ni/Au on n-GaN grown on sapphire and SiC substrates *Appl. Phys. Lett.* **79** 2567–9
[10] Ozbek A M and Baliga B J 2011 Tunneling coefficient for GaN Schottky barrier diodes *Solid State Electron.* **62** 1–4
[11] Yoshizumi Y, Hashimoto S, Tanabe T and Kiyama M 2007 High-breakdown-voltage pn-junction diodes on GaN substrates *J. Cryst. Growth* **298** 875–8
[12] Ahmad M and Arora B M 1992 Investigation of AuGeNi contacts using rectangular and circular transmission line model *Solid State Electron.* **35** 1441–5
[13] Schmitz A C, Ping A T, Khan M A, Chen Q, Yang J W and Adesida I 1996 Schottky barrier properties of various metals on n-type GaN *Semicond. Sci. Technol.* **11** 1464
[14] Iucolano F, Roccaforte F, Giannazzo F and Raineri V 2007 Temperature behavior of inhomogeneous Pt/GaN Schottky contacts *Appl. Phys. Lett.* **90** 092119
[15] Bougrov V, Levinshtein M E, Rumyantsev S L and Zubrilov A 2001 *Properties of Advanced Semiconductor Materials GaN, AlN, InN, BN, SiC, SiGe* (New York: Wiley)
[16] Ozbek A M and Baliga B J 2011 Planar nearly ideal edge-termination technique for GaN devices *IEEE Electron Device Lett.* **32** 300–2
[17] Trivedi M and Shenai K 1999 Performance evaluation of high-power wide band-gap semiconductor rectifiers *J. Appl. Phys.* **85** 6889–97